J Mater Sci (2007) 42:4877–4886
DOI 10.1007/s10853-006-0685-4

Morphological control of Fe_3O_4 particles via glycothermal process

Seung-Beom Cho · Jun-Seok Noh · Sang-Jun Park · Dae-Young Lim · Sang-Heul Choi

Received: 6 October 2005 / Accepted: 19 July 2006 / Published online: 8 March 2007

Abstract Acicular magnetite (Fe_3O_4) powders were synthesized through new glycothermal dehydration by using crystalline α-FeOOH as precursor and glycols as solvent. When ethylene glycol was used as solvent, the phase was in-situ transformed from acicular α-FeOOH to α-Fe_2O_3 and finally to Fe_3O_4 at 270 °C for 6 h without morphological change. When water was added as a co-solvent in glycothermal reaction, Fe_3O_4 powders were synthesized through dissolution–recrystallization process at 230 °C for 3 h. The volume ratio of ethylene glycol to water (E/W) in the reaction has a strong effect on the morphology of the synthesized Fe_3O_4 particles. The particle shape of Fe_3O_4 particles changed from needle to sphere when the water content in E/W volume ratio increased from 0.5 to 1 mL in mixed glycothermal condition. When the water were added by more than 10 ml, the particle shape of Fe_3O_4 changed from sphere to octahedron truncated with the {100} faces and finally distinct octahedron with only {111} faces. Also, it is demonstrated that the size of Fe_3O_4 particles can be controlled from 1–2 μm to 100–200 nm by varying the reaction conditions such as the volume ratio of water to ethylene glycol and additive in glycothermal reaction.

S.-B. Cho (✉) · J.-S. Noh
Corporate R&D, LG Chemical Ltd., Research Park, 104-1, Moonji-dong, Yuseong-gu, Daejeon 305-380, South Korea
e-mail: sebcho@lgchem.com

S.-J. Park · D.-Y. Lim
Department of Inorganic Materials Engineering, College of Engineering, Paichai University, Daejeon, South Korea

S.-H. Choi
Department of Inorganic Materials Engineering, Hanyang University, Seoul, Korea

Introduction

Magnetite (Fe_3O_4) is a representative of the large family of ferrites with spinel structure, which recently has a great attention in the biological and medical diagnostic field [1, 2]. Techniques are being developed to introduce new functions to particulate materials by incorporating magnetic material. Coating of magnetic particles by nonmagnetic materials, coating of nonmagnetic particles by magnetic materials and a combination of enzymes on the surface of magnetic particles have been studied [3, 4]. Inada et al. combined enzymes on synthesized magnetic particles, which can reuse enzymes [4]. Research has been attempted to use magnetic particles in labeling and separation of cells [5]. A magnetic field, induced by the ferrite films, promotes the growth rates for living cells on the surface. This biomagnetic interaction between the ferrite and organism facilitates the fabrication of devices having biologically compatible surfaces [6]. The ferrite coating can be also used as a protective passivation coating for boiler inner walls. The chemical agent used in conventional treatments is potentially toxic due to the use of hydrazine and pollutes the environment due to the use of phosphate ions. Marugame et al. show that the magnetite coating on the boiler wall has a strong corrosion-resistant property [7].

Solution synthesis techniques have the potential to meet the increasing demand for the direct preparation of crystalline ceramic powders and offer a low temperature alternative to conventional powder synthesis techniques in the production of anhydrous oxide powders [8–15]. Solution synthesis techniques can produce fine, high purity, stoichiometric particles of single and multicomponent metal oxides. Furthermore,

if process conditions such as solution pH, solute concentration, reaction temperature, reaction time, and the type of solvent are carefully controlled, ceramic particles of the desired shape and size can be produced.

Many metal oxides and hydroxide particles with narrow size distributions were prepared by Matijevic et al. by forced hydrolysis at elevated temperatures [1, 2, 16–22]. Spherical magnetite particles were formed by phase transformation of precipitated $Fe(OH)_2$ under mild oxidizing conditions in the presence of KNO_3 [18]. Large magnetite particles were also obtained in the presence of chelating agents and reducing agents [19]. Konno et al. prepared magnetite particles using a microemulsion method [23]. In this method, the size of the magnetite particle could be controlled by adjusting the size of water droplets in the microemulsion and the content of ferric and ferrous ions. Nanometer-sized iron oxide particles were prepared using unilamellar vesicles [24]. Adding an alkaline solution to vesicles containing intravesicular solutions of Fe^{2+}, Fe^{3+}, and Fe^{2+}/Fe^{3+} resulted in the formation of membrane-bound discrete particles of goethite, magnetite and ferrihydrite. Hydrothermal synthesis is one of the solution synthesis techniques that are widely used to prepare anhydrous crystalline materials. This method involves the treatment of aqueous solutions or suspensions of precursor materials at elevated temperatures and pressures. The concepts embodied in hydrothermal processing approaches can be extrapolated to nonaqueous systems. However, the reaction mechanisms in nonaqueous solution are complex, and currently there is very limited information regarding the reaction thermodynamics, kinetics, and underlying crystallization mechanisms. Only a few investigations have dealt with the use of organic media to synthesize crystalline ceramic powders [25–31].

The objective of the current work was to prepare uniform Fe_3O_4 particles by the glycothermal method and to establish the processing conditions on the formation, morphology, and phase of the Fe_3O_4 powders. A wet chemical reaction route for the synthesis of Fe_3O_4 was developed by using ethylene glycol. Thus, the formation of phase-pure Fe_3O_4 particles with a variety of specific morphologies via different glycothermal treatments is described.

Materials and methods

The process to prepare Fe_3O_4 particles by glycothermal treatment in glycol solution is schematically illustrated in Fig. 1. All chemicals are reagent grade unless otherwise indicated. Goethite (99%, Junsei Co., Japan)

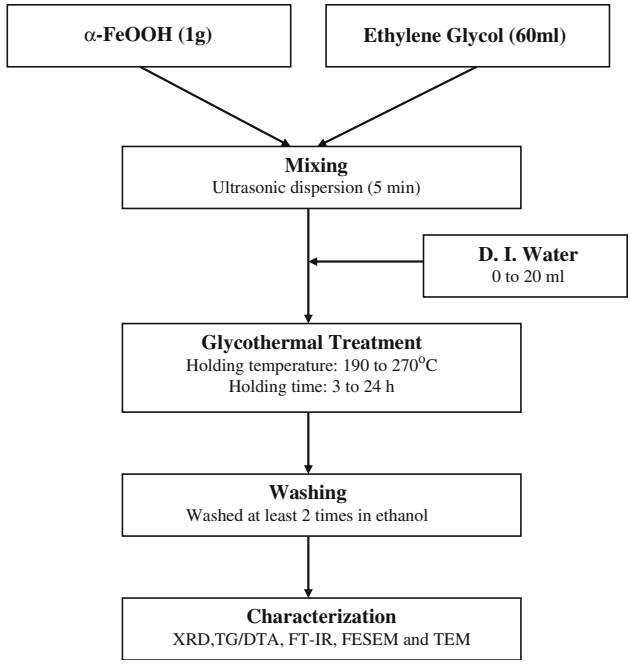

Fig. 1 Schematic representation of processing steps for the preparation of Fe_3O_4 particles in ethylene glycol

was used as a source of Fe, and was used as received. A 1 g of precursor powder was ultrasonically dispersed in 60 mL of ethylene glycol (99%, Shinyo Co., Japan) with vigorous stirring. The resulting suspension was placed in a 100 mL Teflon container which was then placed in a 300 mL stainless steel pressure vessel equipped with a magnetically stirred head (Autoclave Engineer, USA). Additional glycol solution was poured in the gap between the autoclave and the Teflon container. The atmosphere inside the pressure vessel was flushed with nitrogen prior to heating the contents to the desired temperature because glycol solution has a strong tendency to oxidize and decompose at elevated temperature. The reaction time at the desired temperature was varied between 0 and 24 h. The stirring speed under glycothermal conditions was 200 rpm if not specifically mentioned. The autogenous pressure is the spontaneous vapor pressure of the liquid in the vessel, which depends on temperature, the volatility of liquid, and the liquid charge. Therefore, the pressure developed in the vessel is always monitored so as not to exceed the maximum working pressure (20 kgf/cm^2).

After glycothermal treatment, the vessel was cooled to ~30 °C with any residual pressure relieved via a pressure release valve. The solid reaction products were washed at least five times by repeated cycles of centrifugation and redispersion in ethanol. After washing, the recovered powders were dried at 25 °C in

a desiccator for 48 h. The dried, recovered powders were analyzed for phase composition using X-ray diffraction (X-ray diffractometer, CuKα, Fine Tube, 40 kV-40 mA, Rigaku, Japan) over the 2θ range from 10–60° at a scan rate of 7°/min. The morphology of the synthesized particles was observed using scanning electron microscopy (JSM-35CF, JEOL; S-4200, Hitachi, Japan). The internal microstructure of the synthesized particles was observed using transmission electron microscopy (JEM-2000-EX II, JEOL, Japan). Infrared absorption was measured using an FT-IR spectrophotometer (FTS 300, Bio-Rad, USA) for analysis of surface impurities on Fe_3O_4 particles such as C–O and O–H groups and carbonates. Thermogravimetric analysis (TGA) and Differential thermal analysis (DTA) were performed with heating rate of at 2 °C/min up to 1200 °C.

Results and discussion

Glycothermal synthesis of acicular Fe_3O_4 particles in ethylene glycol

The effect of ethylene glycol on the formation of Fe_3O_4 particles under glycothermal conditions was investigated. In order to determine the lowest synthesis temperature, precursors prepared at the conditions for the formation of Fe_3O_4 particles described above were glycothermally treated for 24 h at different temperatures including 190 °C and 210 °C (±2 °C). Phase-pure acicular Fe_3O_4 particles were prepared at temperatures as low as 270 °C for 6 h as shown in Table 1. XRD analysis results show that the phase transformation from α-FeOOH to α-Fe_2O_3 occurs at 210 °C. Thus, the transition temperature of α-FeOOH precursor to intermediate α-Fe_2O_3 phase is in the vicinity of 210 °C and phase-pure α-Fe_2O_3 phase was synthesized at 250 °C for 6 h. The low temperature stable α-Fe_2O_3 phase rearranges its crystal structure and transforms to the higher temperature stable Fe_3O_4 phase at 250 °C. However, α-Fe_2O_3 phase still coexist in the reaction product until the reaction temperature reaches at 270 °C. SEM photomicrographs of Fe_3O_4 particles synthesized at 270 °C are given in Fig. 2.

To study the formation mechanism of α-Fe_2O_3 and Fe_3O_4, the reactions were examined for different reaction times (0–12 h) at 270 °C as shown in Table 2. After a reaction time of 0 h, which means the autoclave was cooled as soon as the reaction temperature reached 270 °C, α-Fe_2O_3 was synthesized. This result indicated that the dehydration reaction of α-FeOOH was predominant and crystallization of hematite proceeded immediately;

$$2\mathrm{FeOOH} \xrightarrow{\text{dehydration}} 2\mathrm{Fe_2O_3} + \mathrm{H_2O} \quad (1)$$

After 1 h, Fe_3O_4 was also observed with α-Fe_2O_3, suggesting that the reduction of hematite to magnetite with ethylene glycol tool place. It is well-known that ethylene glycol in the liquid phase reaction can acts as a solvent as well as a reducing agent [32, 33]. Konishi et al. has reported the reductive formation of magnetite in the liquid phase; the thermal treatment of an

Table 1 Influence of reaction temperature on the formation of Fe_3O_4 particles in ethylene glycol

Sample No.	Reaction temp. (°C)	Reaction time (h)	Amount of precursor	Phase composition	Morphology
EGM-01	190	24	1	α-FeOOH	Acicular
EGM-02	210	24	1	α-Fe_2O_3, α-FeOOH	Acicular
EGM-03	230	24	1	α-Fe_2O_3, α-FeOOH	Acicular
EGM-04	250	6	1	α-Fe_2O_3	Acicular
EGM-05	250	24	1	α-Fe_2O_3, α-Fe_3O_4	Acicular
EGM-06	270	3	1	α-Fe_2O_3, α-Fe_3O_4	Acicular
EGM-07	270	6	1	α-Fe_3O_4	Acicular

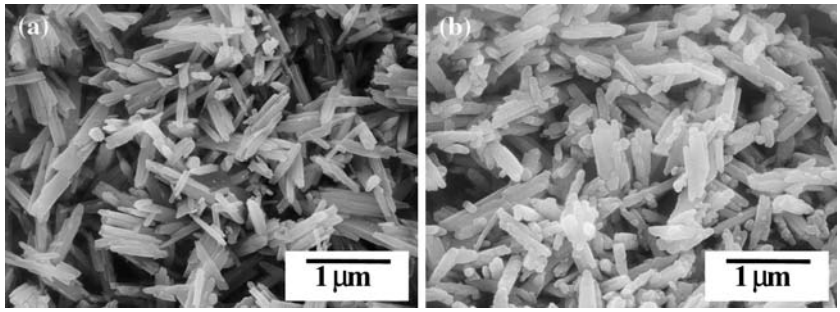

Fig. 2 SEM photomicrographs showing the morphology of Fe_3O_4 particles in glycothermal condition (6 h, 1g α-FeOOH, 60 mL ethylene glycol): (**a**) α-FeOOH precursor and (**b**) 270 °C

Table 2 Influence of reaction time on the formation of Fe_3O_4 particles in ethylene glycol

Sample No.	Reaction temp. (°C)	Reaction time (h)	Amount of precursor (g)	Phase composition	Morphology
EGM-07–01	270	0	1	α-Fe_2O_3	Acicular
EGM-07–02	270	1	1	α-Fe_2O_3, Fe_3O_4	Acicular
EGM-07–03	270	3	1	Fe_3O_4, α-Fe_2O_3	Acicular
EGM-07–04	270	6	1	Fe_3O_4	Acicular
EGM-07–05	270	12	1	Fe_3O_4	Acicular
EGM-07–06	270	24	1	Fe_3O_4	Acicular

iron(III) carboxylate solution at 245 °C yields magnetite by reducing the iron(III) with the organic moieties [34]. Therefore, possible reductive reaction in ethylene glycol is as follows;

$$6Fe_2O_3 \xrightarrow{\text{reduction}} 4FeO \cdot Fe_2O_3 + O_2 \quad (2)$$

This result shows that the phase was in-situ transformed from goethite to hematite, and finally to magnetite without shape change of acicular precursor via dehydration and reductive reactions reaction at 270 °C for 6 h.

Therefore, this processing method provides a simple low temperature solution route for producing acicular Fe_3O_4 particles, which could be used to prepare acicular maghemite (γ-Fe_2O_3) particles for magnetic recording.

Volume ratio of ethylene glycol and water (E/W)

The effect of water on the synthesis temperature and morphology of Fe_3O_4 particles under glycothermal condition was investigated. The XRD analysis results and morphology of the powder synthesized at different water content are given in Table 3 and Fig. 3, respectively. Synthesis temperature of Fe_3O_4 particles decreased from 270 to 210 °C with addition of 10 mL water as a co-solvent as shown Table 2. Also, phase-pure Fe_3O_4 powders were synthesized in the range of E/W volume ratio from 59/1 to 10/50 at 230 °C through glycothermal reaction. Excess water (more than 45/15) causes incomplete reaction in mixed glycothermal condition and the small amount of unreacted intermediate α-Fe_2O_3 phase co-exists in the final product. The particle shape of Fe_3O_4 changed from needle to sphere when the water content in E/W volume ratio increased from 0.5 mL to 1 mL as shown in Fig. 3(a, b). The size of these spherical particles increased from 0.2–0.3 to 1–1.2 μm without morphological change when the water content in E/W volume ratio increased from 1 to 8 mL as shown in Fig. 3 (b–e). Furthermore, when the water were added by more than 10 mL, the particle shape of Fe_3O_4 changed from sphere to octahedron truncated with the {100} faces and finally distinct octahedron with only {111} faces as shown in Fig. 3(f–h). The size of these octahedral particles slightly increased from 1–1.5 to 1.5–2 μm with increasing the water content from 10 to 20 mL. Figure 4 shows the XRD patterns of typical Fe_3O_4 particles with three different shapes. The crystallinity of Fe_3O_4 particles was improved with increasing the water content in E/W volume ratio, which was consistent with the TEM analyses. Based on the results, it is demonstrated that the size and shape of Fe_3O_4 particles can be controlled by simply changing the volume ratio of E/W via mixed glycothermal process. This behavior can be explained by considering the solubility change in mixed glycothermal condition. In general, materials systems with inherently low solubility typically undergo in-situ transformation via dehydration reaction from sparingly soluble precursor materials to polycrystalline agglomerates composed of nanometer-size

Table 3 Influence of water on the formation and morphology of Fe_3O_4 particles in ethylene glycol

Sample No.	Reaction temp. (°C)	Reaction time (h)	Amount of water (mL)	Phase composition	Morphology
EGW-01	190	6	10	α-Fe_2O_3, α-Fe_3O_4	Octahedral
EGW-02	210	6	10	α-Fe_3O_4	Octahedral
EGW-03	230	6	0.5	α-Fe_3O_4, α-Fe_3O_4	Acicular
EGW-04	230	6	1	α-Fe_3O_4	Spherical
EGW-05	230	6	2	α-Fe_3O_4	Spherical
EGW-06	230	6	5	α-Fe_3O_4	Spherical
EGW-07	230	6	8	α-Fe_3O_4	Spherical
EGW-08	230	6	10	α-Fe_3O_4	Truncated octahedral
EGW-09	230	6	15	α-Fe_3O_4, α-Fe_3O_4	Octahedral
EGW-10	230	6	20	α-Fe_3O_4, α-Fe_3O_4	Octahedral

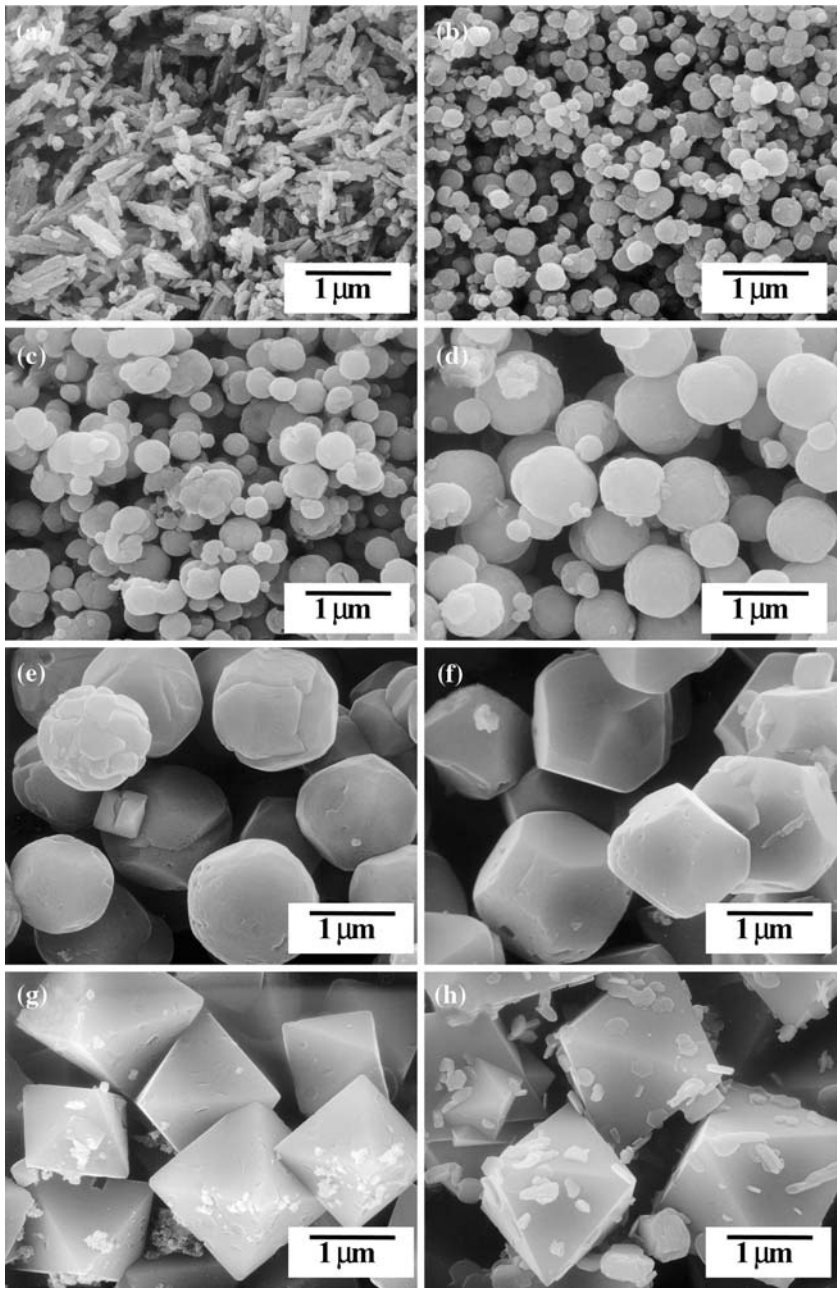

Fig. 3 SEM photomicrographs showing the influence of E/W ratio on the formation and morphology of Fe_3O_4 particles in glycothermal condition (1 g α-FeOOH, 230 °C, 6 h): (**a**) E/W = 60/0, (**b**) E/W = 59/1, (**c**) E/W = 58/2, (**d**) E/W = 55/5, (**e**) E/W = 52/8, (**f**) E/W = 50/10, (**g**) E/W = 45/15, and (**h**) E/W = 40/20

primary particles. Close to the solid-liquid interface, transport is restricted to molecular diffusion through a diffusion boundary layer. The width of the boundary layer, in which transport by molecular diffusion dominates, is a function of the diffusivity of the diffusing species as well as hydrodynamics near the interface. Consequently, the solvent may influence crystal growth through its effect on solubility, viscosity, molecular density, diffusivity, and other heat and mass transport-related properties [35, 36]. Therefore, the phase and even morphology of the resulting crystalline particles can be significantly affected by the chemistry of ethylene glycol. Therefore, it is reasonable to assume that the solubility of α-FeOOH in organic solvent such as ethylene glycol is negligible compared to that of water. Such a solubility of α-FeOOH in ethylene glycol could limit the transport of the solute into the solid-liquid interface for further growth and promotes the nucleation process due to short mean free path of the solute. In this pure glycothermal condition, it is believed that acicular α-FeOOH precursor was in-situ transformed into Fe_3O_4 without morphological change via dehydration reaction in ethylene glycol. The morphological characteristics of the different solid phases

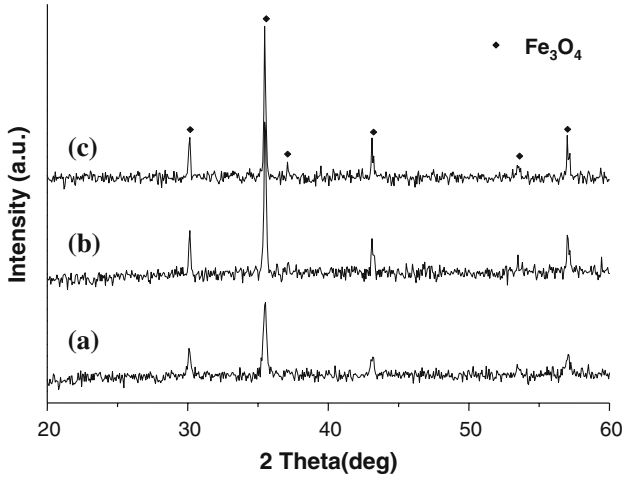

Fig. 4 XRD patterns of typical Fe_3O_4 particles synthesized in glycothermal condition: (**a**) EG-60, (**b**) DI-5, and (**c**) DI-15

involved in pure glycothermal reaction supports that in-situ transformation from α-FeOOH to Fe_3O_4 is dominant in pure glycothermal condition: first, there is no morphological change between the precursor materials and final product as shown in Fig. 2(a, b); second, the Fe_3O_4 particles obtained at the end of the reaction show polycrystalline nature as shown in Fig. 5(a).

In contrast, it is reasonably considered the solubility of FeOOH was increased with increasing the volume ratio of water in mixed glycothermal condition. Morphological evolution of Fe_3O_4 particles from fiber to sphere, finally to octahedron as a function of water volume ratio supports that the solubility difference is enough to change the formation mechanism to in-situ transformation regime to dissolution–recrystalliztion regime. The polycrystalline nature of spherical Fe_3O_4 particles clearly indicates that aggregation mechanism is involved in the formation of the large spheres as shown in Fig. 5(b). The ''raspberry-like'' appearance of spherical Fe_3O_4 particles is strongly reminiscent of the morphology of colloidal aggregates. A successful and revolutionary model for colloidal aggregation was first proposed by Bogush and Zukoski [37] in the context of monodisperse silica particles synthesized by the Stober process [38]. They utilized colloidal science concepts to show that under identical surface charge densities larger particles will attract much smaller particles, whereas particles of similar size will repel one another. This attractive interaction leads to the growth of particle clusters by aggregation and hence a ''raspberry-like'' appearance. Since spherical Fe_3O_4 particles consisted of nanosized primary crystallite as shown in Fig. 5(b), it is expected that spherical Fe_3O_4 particles increases with coagulation of primary crystallite clusters, resulting in a raspberry-like shape which is the characteristic of hydrothermal $BaTiO_3$ particles [39]. Further growth occurs by adhesion of additional primary particles to the already recrystallized spheres.

In the case of high water volume ratio (> 5/55), there are three main features, which must be pointed out in the morphological characteristics of the different solid phases involved in the reaction. First, there is no similarity between the morphologies of the precursor materials and octahedral Fe_3O_4 particles. Second, Fe_3O_4 particles obtained at the end of the reaction exhibit a narrow size distribution. Third, Fe_3O_4 particles obtained at the end of the reaction show single crystalline nature as shown in Fig. 5(c). In general, the different morphologies of the two solid phases involved in the system can only be explained if the transformation of one phase into another proceeds via the solution with dissolution and nucleation-growth steps. A condition that must be fulfilled in order to obtain such particles with a narrow size distribution is the separation of the nucleation and growth steps [40, 41]. This condition has been expressed by La Mer and Dinegar [42] for the preparation of sulfur sol from acidified thiosulfate solutions. In addition, the single crystalline nature of octahedral Fe_3O_4 particles supports that dissolution–recrystallization mechanism is involved in mixed glycothermal conditions as shown in Fig. 5(c). The further growth of octahedral Fe_3O_4

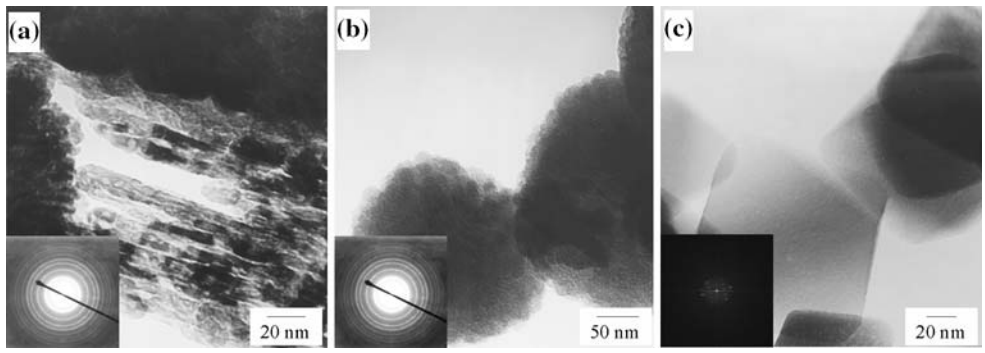

Fig. 5 Bright-field TEM photomicrograph of typical Fe_3O_4 particles synthesized in glycothermal condition: (**a**) EG-60, (**b**) DI-5, and (**c**) DI-15

particles in mixed glycothermal condition could be continued by a solute addition reaction at a rate which promotes consumption of all reactants generated by the dissolution reaction in water without any further nucleation after nucleation of Fe_3O_4 primary crystallite clusters.

Impurities included in the as-prepared Fe_3O_4 particles were investigated by TG/DTA and FT-IR measurements. The magnetite oxidation to hematite is described by Eq. (3).

$$4FeO \cdot Fe_2O_3 + O_2 = 6Fe_2O_3 \quad (3)$$

Impurities included in the as-prepared Fe_3O_4 particles can be reasonably considered with good accuracy by TGA because the total weight gain for the magnetite oxidation to hematite is as large as 3.455 wt% for pure magnetite. Figures 6 and 7 show TGA and DTA analysis of Fe_3O_4 particles at different E/W volume ratio, respectively. The total weight gains between 100 °C and 600 °C are 3.21, 3.10, 2.89 wt% due to the magnetite oxidation to hematite for the samples of EG-60, DI-5 and DI-15, respectively, as shown in Fig. 6. From the TGA analysis, the weight gain of magnetite synthesized in pure glycothermal condition (E/W = 60/0) is close to that of pure magnetite. It is also found that the hydroxyl contents on magnetite particles increased with increasing the water content in glycothermal reaction because the weight loss below 200 °C became more prominent with increasing the water content as shown in Fig. 6. In contrast, the content of chemically bounded glycol groups on magnetic particles decreased with increasing the water content because the intensity of exothermic peaks at 215 °C due to the loss of chemically bounded glycol groups decreased with increasing the water content as shown in Fig. 7. From the TG/DTA results, a topochemical low-temperature oxidation takes place between 200 and 350 °C. At around 400 °C, the second stage of oxidation starts leading to complete oxidation at around 600 to 800 °C, depending on the magnetite samples. Low temperature oxidation is dominant for acicular polycrystalline magnetite sample (EG-60) whereas high-temperature oxidation is dominant for octahedral single crystalline magnetite sample (DI-15) as shown in Fig. 7(a, c). Spherical polycrystalline magnetite sample (DI-5) show the mixed oxidation behavior as shown in Fig. 7(b). The difference in the oxidation behaviors is believed to be due to the different crystallite size of the magnetite samples [43]. Oxidation of magnetite to hematite is a reversible reaction. If the hematite phase is pure, the hematite starts to dissociate back to magnetite with weight loss. These magnetite samples also show different dissociation behaviors due to crystallite size.

This result was consistent with the FT-IR analyses as shown in Fig. 8. The 1520 cm^{-1} band (bending mode of H_2O) indicates that some H_2O is present. The data does reveal weak shoulders near 1050 and 1630 cm^{-1}, which are characterized by the adsorption of CH_2 groups. Chemisoption of ethylene glycol is believed to be involved in the formation of these peaks through substitution on a surface hydroxyl group [44]. The broad band at 574 cm^{-1} is typical of the Fe–O vibrations in Fe_3O_4. FT-IR analyses suggest that several defects are present in the lattice of Fe_3O_4 crystallites.

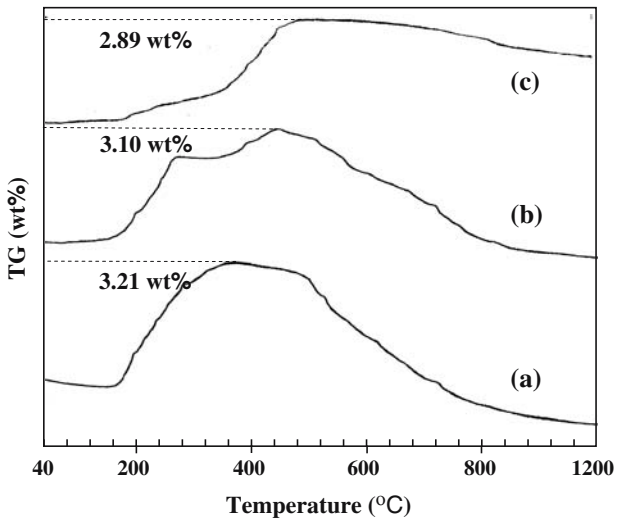

Fig. 6 Thermogravimetric analysis of typical Fe_3O_4 particles synthesized in glycothermal condition: (**a**) EG-60, (**b**) DI-5, and (**c**) DI-15

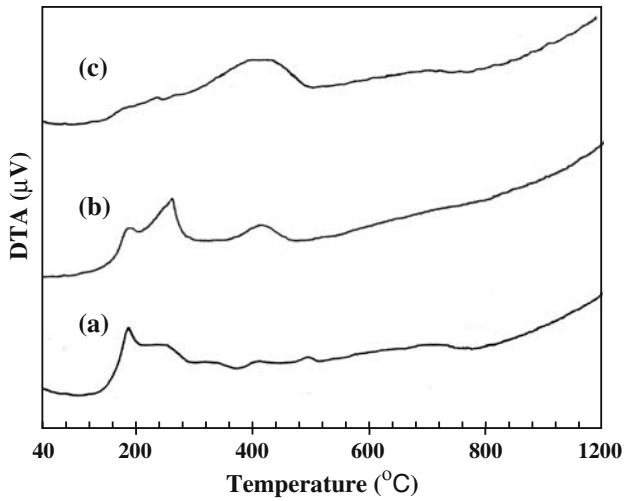

Fig. 7 Differential thermal analysis of typical Fe_3O_4 particles synthesized in glycothermal condition: (**a**) EG-60, (**b**) DI-5, and (**c**) DI-15

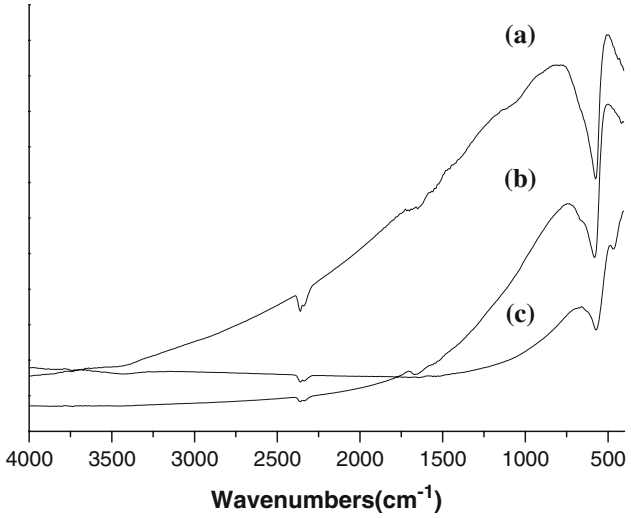

Fig. 8 FT-IR spectra of typical Fe_3O_4 particles synthesized in glycothermal condition: (**a**) EG-60, (**b**) DI-5, and (**c**) DI-15

Influence of additives

In a solution environment, unlike in vapor, the solvent is not inert but assumes some role in the particle formation. Solvent–solid interactions modify the surface energy and hence influence the shape of the crystal. Specific adsorption of ions, complexes, and organic compounds may also affect morphology by restraining, or sometimes promoting, the growth of the faces onto which such species are adsorbed. Besides, the iron precursor, it is possible to use cationic or anionic additives, which are able to have an important influence on the morphology of the resulting particles. Therefore, the effects of the additives on the morphology of Fe_3O_4 particles in ethylene glycol are evaluated. It was shown earlier that small amount of citric acid has a significant effect on the morphology of hematite particles produced in aqueous solution [45]. Citric acid was adsorbed in the form of citrate anion ($RCOO^-$) on the ferric hydroxide and produce the needle-like α-Fe_2O_3 particles. However, when citric acid was added as growth-directing agent in glycothermal condition, the size and shape of Fe_3O_4 particles became irregular as shown in Fig. 9. These results indicate that citric acid is unstable at 230°C in glycothermal condition and the dehydration and decomposition of citric acid into itaconic acid extensively occurs at the glycothermal condition as shown in Fig. 10. This extensive dehydration and decomposition of citric acid is believed to change the adsorption properties in glycothermal conditions and cause the different nucleation and growth of Fe_3O_4 particles.

In the case of the itaconic acid, which is a final decomposition product of citric acid, it is possible to control the particle size of Fe_3O_4 particles without morphological change. The size of the spherical particles decreased from 0.5–1 μm to 100–200 nm without morphological change when the concentration of itaconic acid increased from 10^{-3} to 5×10^{-2} M as shown in Fig. 11(a–c). Also, the particle size of octahedral Fe_3O_4 decreased from 0.5–1 to 0.3–0.5 μm without morphological change when the concentration of itaconic acid increased from 10^{-2} to 5×10^{-2} M as shown in Fig. 11(d, e). Finally, the particle shape of Fe_3O_4 changed from octahedron to sphere when the concentration of itaconic acid is 10^{-1} M as shown in Fig. 11(f). The size of Fe_3O_4 particles decreased from 300–500 to 100–150 nm. This result indicated that itaconic acid increases the supersaturation level, thus increasing nucleation frequency, and subsequently reducing the particle size of Fe_3O_4 particles in glycothermal conditions

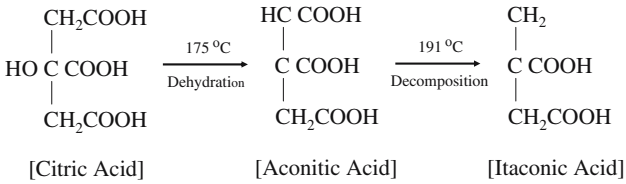

Fig. 10 Dehydration and decomposition mechanism of citric acid

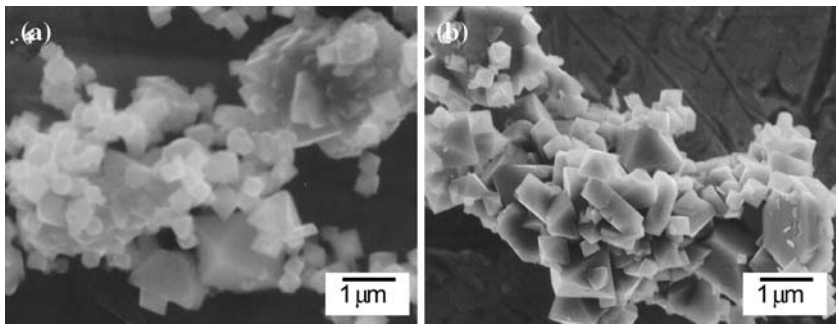

Fig. 9 SEM photomicrographs showing the influence of citric acid on the formation and morphology of Fe_3O_4 particles in glycothermal condition (230 °C, 6 h, 1 g α-FeOOH): (**a**) 10^{-3} M citric acid, E/W = 50/10 and (**b**) 10^{-3} M citric acid, E/W = 40/20

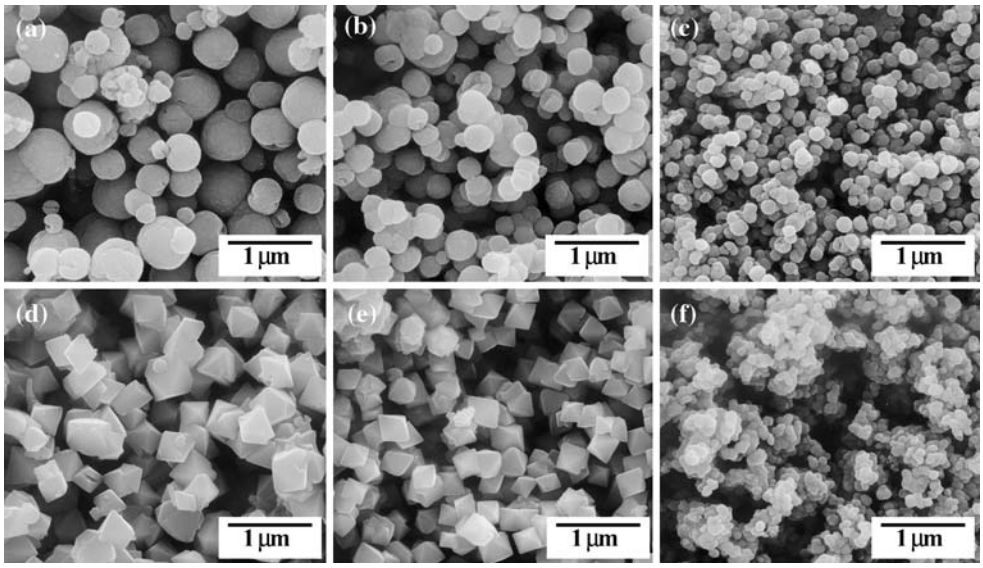

Fig. 11 SEM photomicrographs showing the influence of itaconic acid on the formation and morphology of Fe_3O_4 particles in glycothermal condition (230 °C, 6 h, 1 g α-FeOOH): (**a**) 10^{-3} M itaconic acid, E/W = 55/5 and (**b**) 10^{-2} M itaconic acid, E/W = 55/5, (**c**) 2×10^{-2} M itaconic acid, E/W = 55/5, (**d**) 10^{-2} M itaconic acid, E/W = 50/10, (**e**) 5×10^{-2} M itaconic acid, E/W = 50/10, and (**f**) 10^{-1} M itaconic acid, E/W = 50/10

Conclusion

Fe_3O_4 particles with different size and shape have been synthesized by glycothermal treatment of α-FeOOH precursors under autogenous vapor pressures. Present work shows that the in-situ phase transformation occurs from acicular α-FeOOH to α-Fe_2O_3 and finally Fe_3O_4 at 270 °C without morphological change when glycol was used as a solvent. However, the formation mechanism is changed from in-situ transformation to dissolution–recrystallization process and the morphology of Fe_3O_4 particles is changed from fiber to sphere, finally to octahedron as a function of E/W volume ratio. Furthermore, it is demonstrated that the size of Fe_3O_4 particles can be controlled from 1–2 μm to 100–200 nm by varying the reaction conditions such as the volume ratio of water to ethylene glycol and additive in glycothermal reaction.

References

1. Pieters BR, Williams RA, Webb C (1992) In: Williams RA (ed) Colloid and surface engineering. Butterworth-Heinemann, Oxford, p 248
2. Ozaki M (1994) In: Lee BI, Pope WJA (eds) Chemical processing of ceramics. Marcel Dekker, Inc., New York, p 421
3. Ochiai K, Horie H, Kamohara H, Morita M (1987) Nippon Kagaku Kaishi 233
4. Inada Y, Takahashi K, Yoshimoto T, Kodera Y, Matsushima A, Saito Y (1988) Trends Biotechnol 6:131
5. Molday RS, Yen SPS, Rembaum A (1977) Nature 268:437
6. Egusa K, Marugame K, Abe M, Itoh T (1992) In: Proceedings of the Sixth International Conference on Ferrites (ICF-6). Tokyo and Kyoto, Japan, p 11
7. Marugame K, Egusa K, Abe M (1992) In: Proceedings of the Sixth International Conference on Ferrites (ICF-6). Tokyo and Kyoto, Japan, p 1720
8. Matijevic′ E (1987) In: Vincenzini P (ed) Materials science monographs, vol 38A. High Tech Ceramics Part A. Elsevier Science Publishers B.V., New York, p 441
9. Matijevic′ E (1992) In: Hench LL, West JK (eds) Chemical processing of advanced materials. John Wiley and Sons, Inc., p. 513
10. Sugimoto T (1987) Adv Colloid Interface Sci 28:65
11. Somiya S (1989) Hydrothermal reaction for materials science and engineering: An overview of research in Japan. Elsevier Science Publishers Ltd., New York, NY
12. Hirano S (1987) Am Ceram Soc Bull 66(9):1342
13. Dawson WJ (1989) Am Ceram Soc Bull 67(10) 1673
14. Segal D (1989) In: Chemical synthesis of advanced ceramic materials. Cambridge University Press, Cambridge, p 114
15. Abe K, Matsumoto S (1991) In: Hirano S, Messing GL, Hausner H (eds) Ceramic transactions, vol 22, Ceramic Powder Science, vol IV. The American Ceramic Society, Inc., Columbus, Ohio, p 15
16. Matijevic′ E, Scheiner P (1978) J Colloid Interface Sci 63:509
17. Ozaki M, Krathovil S, Matijevi E (1984) J Colloid Interface Sci 102:145
18. Sugimoto T, Matijevi E (1980) J Colloid Interface Sci 74:227
19. Hamada S, Matijevi E (1981) J Colloid Interface Sci 84:274
20. Ozaki M, Ookoshi N, Matijevi E (1990) J Colloid Interface Sci 137:546
21. Blesa MA, Matijevic′ E (1989) Adv Colloid Interface Sci. 29:173
22. Matijevic′ E, Cimas S (1987) Colloid Polym Sci 265:155
23. Gobe M, Konno K, Kandori K, Kitahara A (1983) J Colloid Interface Sci 93:293
24. Mann S, Hannington JP (1988) J Colloid Interface Sci 122:326
25. Dubois T, Demazeau G (1994) Mater Lett 19:38
26. Fanelli AJ, Burlew JV (1986) J Am Ceramic Soc 69(8):C174
27. Inoue M, Tanino H, Kondo Y, Inui T (1989) J Am Ceramic Soc 72(2):352
28. Inoue M, Otsu H, Kominami H, Inui T (1991) J Am Ceramic Soc 74(6):1452

29. Cho SB, Venigalla S, Adair JH (1995) In: Adair JH, Casey JA, Randall CA, Venigalla S (eds) Ceramic transaction, vol 54, Science, technology, and applications of colloidal suspensions. American Ceramic Society, Westerville, OH, p 139
30. Cho SB, Venigalla S, Adair JH (1996) J Am Ceramic Soc 79(1):88
31. Bell NE, Cho SB, Adair JH (1998) J Am Ceramic Soc 81(6):1411
32. Sun Y, Xia Y (2002) Science 298:2176
33. Lim PY, Liu RS, She PL, Hung CF, Shih HC (2006) Chem Phys Lett 420:305
34. Kominami H, Onoue S, Matsuo K, Kere Y. (1999) J Am Ceramic Soc 82(7):1937
35. Mullin JW (1979) In: de long EJ, Jancic SJ (eds) Industrial crystallization 78. North-Holland, Amsterdam, p 93
36. Randolph AD, Larson MA (1988) In: Theory of particulate processes: Analysis and techniques of continuous crystallization. Academic Press, Inc., San Diego, CA, p 109
37. Bogush GH, Zukoski CF IV (1988) In: Mackenzie JD, Ulrich DR (eds) Ultrastructure processing of advanced ceramics. John Wiley & Sons, Inc., New York, p 477
38. Stober W, Fink A, Bohn E (1968) J Colloid Interface Sci 26:62
39. Chien AT, Speck JS, Lange FF, Daykin AC, Levi CG (1995) J Mater Res 10(7):1784
40. Overbeek JTG (1982) Adv Colloid Interface Sci 15:251
41. Sugimoto T (1987) Adv Colloid Interface Sci 28:65
42. La Mer VK, Dinegar RH (1950) J Am Chem Soc 72:4847
43. Forsmo SPE, Hägglund A (2003) Int J Mineral Process 70:109
44. Morrow BA (1980) In: Bell AT, Hair ML (eds) Vibrational spectroscopies for adsorbed species, ACS Symposium Series, vol 137. American Chemical Society, Washington, DC, p 119
45. Byeon TB, Sohn JG (1996) Korean J Mater Res 6(8):768